HAL
open science

Regional contribution to variability and trends of global gross primary productivity

Min Chen, Rashid Rafique, Ghassem Asrar, Ben Bond-Lamberty, Philippe Ciais, Fang Zhao, Christopher Reyer, Sebastian Ostberg, Jinfeng Chang, Akihiko Ito, et al.

To cite this version:

Min Chen, Rashid Rafique, Ghassem Asrar, Ben Bond-Lamberty, Philippe Ciais, et al.. Regional contribution to variability and trends of global gross primary productivity. Environmental Research Letters, 2017, 12 (10), 10.1088/1748-9326/aa8978 . hal-01832898

HAL Id: hal-01832898

https://hal.science/hal-01832898v1

Submitted on 16 May 2021

HAL is a multi-disciplinary open access archive for the deposit and dissemination of scientific research documents, whether they are published or not. The documents may come from teaching and research institutions in France or abroad, or from public or private research centers.

L'archive ouverte pluridisciplinaire **HAL**, est destinée au dépôt et à la diffusion de documents scientifiques de niveau recherche, publiés ou non, émanant des établissements d'enseignement et de recherche français ou étrangers, des laboratoires publics ou privés.

ENVIRONMENTAL RESEARCH
LETTERS

LETTER • OPEN ACCESS

Regional contribution to variability and trends of global gross primary productivity

To cite this article: Min Chen *et al* 2017 *Environ. Res. Lett.* **12** 105005

View the article online for updates and enhancements.

Related content

- Photosynthetic productivity and its efficiencies in ISIMIP2a biome models: benchmarking for impact assessment studies
  Akihiko Ito, Kazuya Nishina, Christopher P O Reyer et al.
- Benchmarking carbon fluxes of the ISIMIP2a biome models
  Jinfeng Chang, Philippe Ciais, Xuhui Wang et al.
- Climate data induced uncertainty in model-based estimations of terrestrial primary productivity
  Zhendong Wu, Anders Ahlström, Benjamin Smith et al.

Recent citations

- Spatiotemporal Patterns of Ecosystem Restoration Activities and Their Effects on Changes in Terrestrial Gross Primary Production in Southwest China
  Zhi Ding *et al*
- Water use efficiency in terrestrial ecosystem over East Asia: Effects of climate regimes and land cover types
  Daeun Kim *et al*
- Optimization of Multi-Ecosystem Model Ensembles to Simulate Vegetation Growth at the Global Scale
  Linling Tang *et al*

This content was downloaded from IP address 86.246.146.51 on 16/05/2021 at 11:05

Environmental Research Letters

OPEN ACCESS

RECEIVED
30 November 2016

REVISED
16 August 2017

ACCEPTED FOR PUBLICATION
31 August 2017

PUBLISHED
28 September 2017

Original content from this work may be used under the terms of the Creative Commons Attribution 3.0 licence.

Any further distribution of this work must maintain attribution to the author(s) and the title of the work, journal citation and DOI.

LETTER

Regional contribution to variability and trends of global gross primary productivity

Min Chen[1,15], Rashid Rafique[1], Ghassem R Asrar[1], Ben Bond-Lamberty[1], Philippe Ciais[2], Fang Zhao[3], Christopher P O Reyer[3], Sebastian Ostberg[3,4], Jinfeng Chang[5], Akihiko Ito[6], Jia Yang[7], Ning Zeng[8], Eugenia Kalnay[8], Tristram West[9], Guoyong Leng[1], Louis Francois[10], Guy Munhoven[10], Alexandra Henrot[10], Hanqin Tian[7], Shufen Pan[7], Kazuya Nishina[7], Nicolas Viovy[5], Catherine Morfopoulos[11], Richard Betts[11,12], Sibyll Schaphoff[3], Jörg Steinkamp[13] and Thomas Hickler[13,14]

1 Joint Global Change Research Institute, Pacific Northwest National Laboratory, College Park, MD, United States of America
2 Laboratoire des Sciences du Climat et de l'Environnement, UMR8212, CEA-CNRS-UVSQ, 91191 Gif-sur-Yvette, France
3 Potsdam Institute for Climate Impact Research, D-14412 Potsdam, Germany
4 Geography Department, Humboldt-Universität zu Berlin, Unter den Linden 6, D-10099 Berlin, Germany
5 Sorbonne Universités (UPMC, Univ Paris 06)-CNRS-IRD-MNHN, LOCEAN/IPSL, 4 place Jussieu, 75005 Paris, France
6 National Institute for Environmental Studies, Tsukuba, Ibaraki 3058506, Japan
7 International Center for Climate and Global Change Research, and School of Forestry and Wildlife Sciences, Auburn University, Auburn, AL 36849, United States of America
8 Department of Atmospheric and Oceanic Sciences, University of Maryland College Park, MD 20742, United States of America
9 Joint Global Change Research Institute, Pacific Northwest National Laboratory, College Park, MD, United States of America
10 UR—SPHERES, Université de Liège, B-4000 Liège, Belgium
11 College of Life and Environmental Sciences, University of Exeter, Exeter EX4 4QF, United Kingdom
12 MetOffice, Hadley Centre, Exeter EX1 3PB, United Kingdom
13 Senckenberg Biodiversity and Climate Research Centre (BiK-F), Senckenberganlage 25, 60325 Frankfurt am Main, Germany
14 Goethe University, Department of Physical Geography, Altenhöferallee 1, 60438 Frankfurt am Main, Germany
15 Author to whom any correspondence should be addressed.

E-mail: min.chen@pnnl.gov

Keywords: gross primary productivity, terrestrial ecosystems, inter-annual variability, seasonal variability

Supplementary material for this article is available online

Abstract

Terrestrial gross primary productivity (GPP) is the largest component of the global carbon cycle and a key process for understanding land ecosystems dynamics. In this study, we used GPP estimates from a combination of eight global biome models participating in the Inter-Sectoral Impact-Model Intercomparison Project phase 2a (ISIMIP2a), the Moderate Resolution Spectroradiometer (MODIS) GPP product, and a data-driven product (Model Tree Ensemble, MTE) to study the spatiotemporal variability of GPP at the regional and global levels. We found the 2000–2010 total global GPP estimated from the model ensemble to be 117 ± 13 Pg C yr^{-1} (mean $\pm$ 1 standard deviation), which was higher than MODIS (112 Pg C yr^{-1}), and close to the MTE (120 Pg C yr^{-1}). The spatial patterns of MODIS, MTE and ISIMIP2a GPP generally agree well, but their temporal trends are different, and the seasonality and inter-annual variability of GPP at the regional and global levels are not completely consistent. For the model ensemble, Tropical Latin America contributes the most to global GPP, Asian regions contribute the most to the global GPP trend, the Northern Hemisphere regions dominate the global GPP seasonal variations, and Oceania is likely the largest contributor to inter-annual variability of global GPP. However, we observed large uncertainties across the eight ISIMIP2a models, which are probably due to the differences in the formulation of underlying photosynthetic processes. The results of this study are useful in understanding the contributions of different regions to global GPP and its spatiotemporal variability, how the model- and observational-based GPP estimates differ from each other in time and space, and the relative strength of the eight models. Our results also highlight the models' ability to capture the seasonality of GPP that are essential for understanding the inter-annual and seasonal variability of GPP as a major component of the carbon cycle.

© 2017 The Author(s). Published by IOP Publishing Ltd

1. Introduction

Terrestrial ecosystems play a critical role in the global carbon cycle (Le Quéré *et al* 2016). Gross primary productivity (GPP), the carbon uptake by terrestrial ecosystems through plant photosynthesis, is the largest global CO_2 flux (Le Quéré *et al* 2016) and the major driver of many ecosystem processes. Therefore, it is important to understand the spatiotemporal variability of GPP for obtaining reliable estimates of terrestrial ecosystems capacity to serve as a major reservoir for carbon, especially in light of continued buildup of atmospheric carbon dioxide in the atmosphere for the rest of this century (Ciais *et al* 2013).

The spatial and temporal variations of global GPP are controlled by climate conditions, vegetation types and their spatial distribution, the nutrient availability, and other factors such as land-use practice that affect the distribution and composition of ecosystems (Ahlström *et al* 2015). Modeling studies suggest large differences in different approaches used to obtain estimates of global GPP (Anav *et al* 2013), largely controlled by seasonal, decadal and longer time variability and change in different regions, globally (Ahlström *et al* 2015). Many studies have estimated GPP in key regions of the world: for example, Lee *et al* (2013) estimated GPP in Amazonia using Greenhouse gases Observing SATellite (GOSAT) measurements; Liu *et al* (2014) estimated GPP in China using five GPP models and Moderate Resolution Imaging Spectroradiometer (MODIS) observations; Jung *et al* (2008) estimated GPP in Europe (EU) using terrestrial ecosystem models; Nightingale *et al* (2008) and Chen *et al* (2011) estimated GPP in the USA using MODIS observations; and Friedlingstein *et al* (2010) estimated GPP in the Sahel region of Africa using ORCHIDEE model. In spite of this large body of research, there is limited information on the relative contributions of these regions to the seasonal, inter-annual and longer time variability of total global GPP.

One significant challenge is that GPP cannot be directly measured (Ma *et al* 2015). The most common methods for estimating regional and global GPP include using remote sensing data, statistical interpolation, and process-based carbon cycle model simulations. For example, the MODIS GPP estimate is derived from satellite-based observations and a light-use efficiency algorithm (Running *et al* 2004); the Model Tree Ensemble GPP (MTE GPP) product is derived from eddy covariance flux measurements by the global FLUXNET network and the parameterization of the relationship between GPP and the explanatory variables (Jung *et al* 2011, Beer *et al* 2010). Generally, good spatiotemporal correlation between site-level inferred GPP and MODIS-based estimates as well as MTE products has been reported in literature (Sjöström *et al* 2013, Zhu *et al* 2016, Gebremichael and Barros 2006, Turner *et al* 2006), and these products have been widely used for analyzing spatiotemporal variation of global GPP, and for benchmarking the process-based model estimates of GPP.

With common simulation protocols, and consistent input data, model intercomparison projects (MIPs) have been launched to analyze terrestrial ecosystem model outputs (e.g. GPP) in a systematic fashion, improve models' estimates, and facilitate model improvement. The recent Inter-Sectoral Impact Model Intercomparison Project (ISIMIP) provides a framework for developing and using such a common modeling protocol by a number of models, and offer a unique opportunity to use their simulated results to better understand the spatial, inter-annual and seasonal variation of GPP at regional and global scales (Warszawski *et al* 2014). These models serve as an important and alternative way to estimate GPP variation for a range of spatial and temporal scales, and in response to multiple environmental factors (Ahlström *et al* 2015, Xia *et al* 2015). However, as indicated by previous MIPs, such as the Multi-scale synthesis and Terrestrial Model Intercomparison Project (MsTMIP) (Huntzinger *et al* 2013) and TRENDY (Sitch *et al* 2008), the magnitude and patterns of model-estimated GPP varies largely across the models, indicating limited understanding of the fundamental underlying ecological process.

In this study, we used a combination of GPP products from MODIS and MTE GPP, and those simulated by eight ISIMIP Phase 2a (ISIMIP2a) terrestrial biome models to understand the contribution of terrestrial ecosystems to carbon cycle under the historical conditions, for the 1971–2010 period. Our main objectives were to: (1) report the ISIMIP2a model-estimated GPP and evaluate the ISIMIP2a models' performance against MODIS and MTE-GPP; (2) examine the spatial, inter-annual and seasonal variability of GPP at global and regional scales; and (3) assess the relative contribution of major regions to the global GPP.

2. Methods

2.1. Data

The MODIS GPP (MOD17) (Zhao and Running 2010) is the first satellite-based modeled dataset for monitoring vegetation productivity at the global scale. A light use efficiency model is the core of MODIS GPP algorithm (Running *et al* 2004). The MODIS GPP data is available for 8 day, monthly and annual timescales at 1 km and $0.05° \times 0.05°$ spatial resolution since 2000, and we analyzed the data for 2000–2010 period in this study. The MODIS GPP products were resampled to $0.5° \times 0.5°$ resolution by area-weighted averaging of the values in each 10×10 pixel window from the original $0.05° \times 0.05°$ product.

The MTE-GPP product (Jung *et al* 2009, 2011) was upscaled based on the globally distributed FLUXNET eddy-covariance tower measurements with a 'Model Tree Ensembles' machine-learning algorithm. The MTE-GPP is currently available as a monthly

Table 1. The major processes represented in eight ISIMIP terrestrial biome models.

Model	Time step	# of soil layers	N cycle	GPP model	Leaf to canopy	Phenology	Phenology cont.	Water stress affect	Heat stress affect	Closed energy balance	Fire	Reference
CARAIB	Daily	1	No	EK	3 leaf	Dyn.	Moist, Temp	Photo, Pheno, Heter. Resp.	Photo, resp	Yes	Yes	(Dury *et al* 2011)
DLEM	Daily	10	Yes	EK	2 leaf	Semi-Prog	GDD	Photo, C alloc, ET, biogeochem	Photo, resp	No	No	(Tian *et al* 2010, 2015, Pan *et al* 2014)
JULES	Hourly	4	No	EK	2 leaf	Dyn.	Temp	Photo, resp	No	Yes	No	(Clark *et al* 2011)
LPJmL	Daily	5	No	EK	1 leaf	Semi-Prog	GDD	Photo, C alloc, ET, biogeochem	Photo, resp	Yes	Yes	(Bondeau *et al* 2007)
LPJ-GUESS	Daily	2	Yes	EK	x leaf	Dyn.	Moist, Temp	Photo, C alloc, ET, biogeochem	Photo, resp	No	Yes	(Smith *et al* 2001)
ORCHIDEE	Half-hourly	11	No	EK	1 leaf	Prog.	Moist, Temp	Photo, pheno	Pheno	Yes	No	(Krinner *et al* 2005)
VEGAS	Daily	2	No	LUE	1 leaf	Dyn.	Moist, Temp	Photo, C alloc, ET, biogeochem	No	Yes	Yes	(Zeng *et al* 2005)
VISIT	Monthly	2	No	EK	1 leaf	Semi-Prog	GDD	Photo, ET, pheno, biogeochem	Photo, resp.	No	Yes	(Ito and Inatomi 2011)

EK = enzyme kinetic, LUE = light use efficiency, BL = Big-Leaf model including stomatal gas exchange regulation, ET = evapotranspiration, GDD = growing degree days, Dyn = dynamic, Semi-Prog. = semi-prognostic, Moist = moisture, Temp = temperature, Phen. = phenology, Photo = photosynthesis, C = carbon, alloc = allocation, Prog = prognostic, x leaf = no specific leaf layers as it is a gap model with age cohorts of different age/heights.

product at 0.5° × 0.5° resolution for 1982–2011 period, and we used the 1982–2010 data in this study.

We used eight ISIMIP2a biome models: CARAIB, DLEM, JULES, LPJmL, LPJ-GUESS, ORICHIDEE, VEGAS, and VISIT from the ISIMIP Phase 2a project. A summary of underlying processes for these models is presented in table 1. We used the simulated GPP from these eight models for 1971–2010 period, all at 0.5° × 0.5° spatial resolution. We calculated the mean GPP from the eight models (hereafter 'ENSEMBLE'). The models' simulations were performed using the common ISIMIP2a protocol, including time variant CO_2 concentrations, climate forcing, and land use change data. All models used the same climate forcing data from Global Soil Wetness Project 3 (GSWP3). More details of ISIMIP2a models are in the supplementary material available at stacks.iop.org/ERL/12/105005/mmedia, and more information about the models' simulation protocol and input data are available at www.isimip.org/protocol/#isimip2a.

2.2. Analysis

We divided the global land area into 12 regions (figure 1) by considering their climate, land cover and geopolitical characteristics: Boreal North America (BNA), Temperate North America (TNA), Tropical Latin America (TLA), Temperate South America (TSA), Europe (EUR), Semi-arid and Arid Asia-Europe-Africa (SAAEA), Tropical Africa (TAF), South Africa (SA), Boreal Euro-Asia (BEA), Temperate Asia (TEA), Tropical Asia (TA) and Oceania (OCE). We calculated the temporal trend of GPP for the annual global and regional GPP (area-weighted) using linear least square regression method. *F*-statistic was used to test the significance of the linear trend. GPP anomaly was calculated as the departure of the long-term mean of the detrended annual-GPP. The GPP inter-annual variability (IAV) for each region and the entire globe was calculated as the standard deviation of the detrended annual GPP at each of these spatial scales. We compared the IAV of ISIMIP2a model estimated GPP against MODIS and MTE by calculating the Pearson's correlation coefficient (R), with the detrended annual GPP. For each region and the entire globe, we calculated the mean monthly GPP to analyze the seasonal variations, which are also compared across ISIMIP2a models, MODIS and MTE with the Pearson's correlation coefficient. We also calculated each region's relative contribution to global GPP trend, seasonality and IAV based on the method from Ahlström *et al* (2015) (see supplementary material for details). The Matlab R2016b was used for all statistical analysis.

3. Results

3.1. Spatial pattern of global GPP

The spatial pattern of GPP from MODIS, MTE and ENSEMBLE generally agree well (figure 2). The highest GPP values are in tropical regions (e.g. Amazonia, Central Africa and Southeast Asia) because of the wet and humid climate; and, the lowest GPP values are mainly in the arid regions of North Africa, West Asia and South

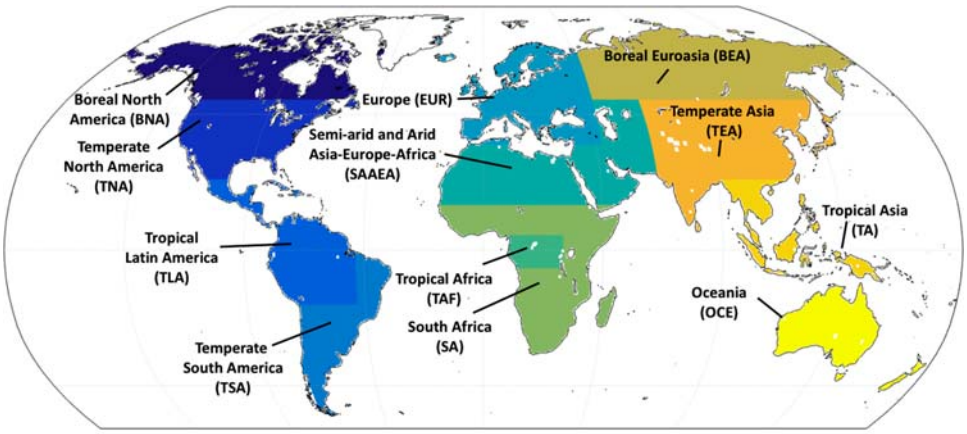

Region	BNA	TNA	TLA	TSA	EUR	SAAEA	TAF	SA	BEA	TEA	TA	OCE
Area (Mkm^2)	9.56	10.1	11.2	8.12	9.53	17.4	2.66	16.7	14.7	17.2	4.88	7.96

Figure 1. Global land regions used in this study.

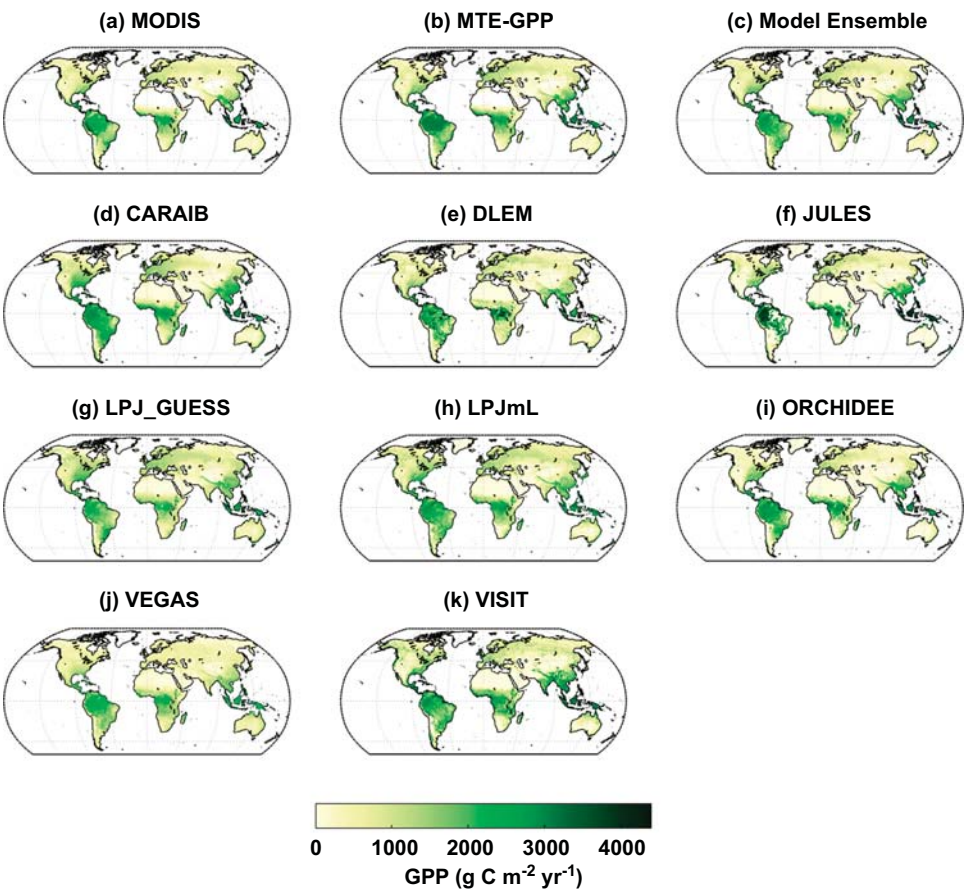

Figure 2. Annual global terrestrial ecosystems gross primary production (GPP) from MODIS (2000–2010), MTE (1982–2010) and ISIMIP models (1971–2010).

America, as well as the cold and snow-covered regions (e.g. Greenland), due to the unfavorable conditions for plant photosynthesis. However, the representation of this variability by eight models was different, with JULES and DLEM producing exceptionally high GPP in tropical regions, especially in Amazonia and the Sahel, while CARAIB producing high GPP in the temperate regions.

Over the 2001–2010 period, the eight models' estimates diverge in total global GPP, ranging from 106 (ORCHIDEE) to 134 (VISIT) $Pg\,C\,yr^{-1}$ (figure 3(*a*), figure S1a), with a standard deviation of

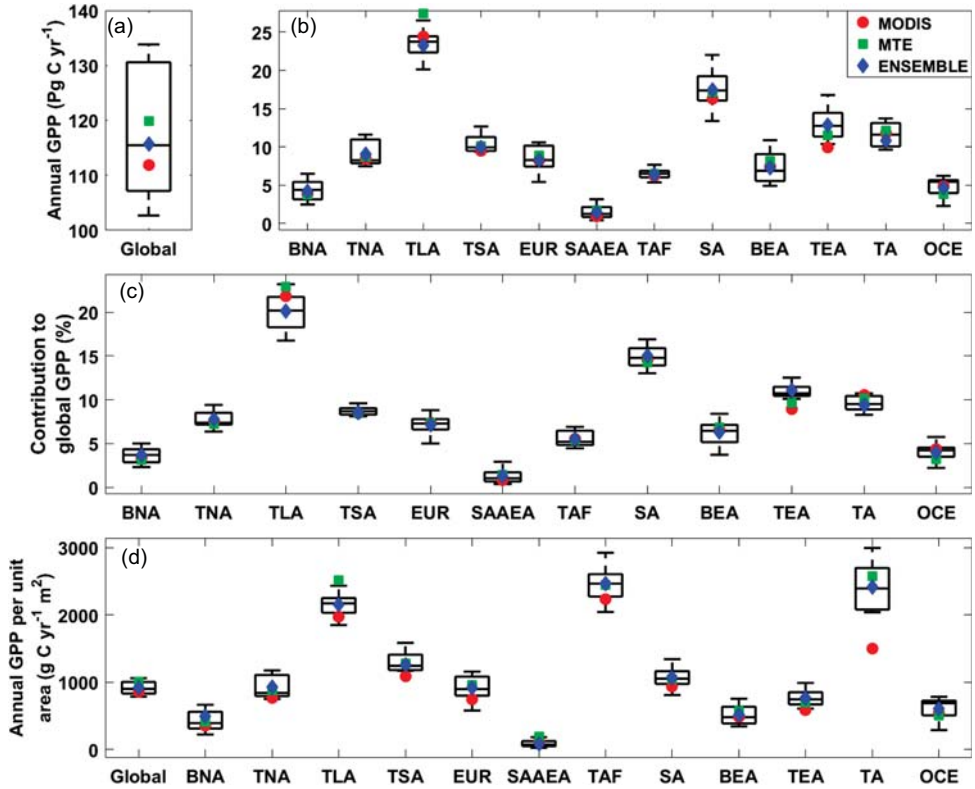

Figure 3. Global and regional annual GPP. The red, green and blue markers represent MODIS, MTE and the model ensemble mean (ENSEMBLE), respectively. Boxplots show the distributions of the eight ISIMIP models. Horizontal lines in the boxplots from top to bottom indicate the 95th, 75th, 50th, 25th, and 5th percentiles. (*a*) and (*b*) show the annual mean global and regional GPP; (*c*) contributions to global GPP from each region; (*d*) annual mean GPP per unit square meters. All of the results shown in this figure are for the period of 2000–2010. Regions abbreviations used on the *x*-axes are defined in figure 1.

13 Pg C yr^{-1}. The ENSEMBLE estimate of total global GPP is 118 Pg C yr^{-1}, which is higher than MODIS estimate of 112 Pg C yr^{-1} but lower than MTE estimate of 120 Pg C yr^{-1} (figure 3(*a*)). Based on the ENSEMBLE estimates (figure 3(*b*)), the regional sum of GPP in Tropical Latin America is the highest among all 12 regions (23 Pg C yr^{-1}), followed by Southern Africa (17 Pg C yr^{-1}) and Temperate Asia (13 Pg C yr^{-1}). The top three regions together contribute about 45% to global GPP (figure 3(*c*)). However, GPP estimates per unit area are the highest in tropical regions (Tropical Africa, Tropical Asia and Tropical South America) with > 2000 g C m^{-2} yr^{-1} (figure 3(*d*)). The regional contributions to global GPP from MODIS and MTE show similar patterns to the ISIMIP2a models based estimates.

3.2. Trend and regional contributions

The ENSEMBLE global GPP increased from 105 Pg C yr^{-1} in 1971 to 118 Pg C yr^{-1} in 2010, with a significant trend of 0.28 Pg C yr^{-2} ($p < 0.01$, figure 4). During 1971–2010, all regions except Oceania show significant increasing trends in GPP, with the fastest rates of increase in Boreal Euro-Asia and Temperate Asia (both 0.04 Pg C yr^{-2}). The trend of the ensemble mean is similar to the trends of individual GPP from the eight ISIMIP2a models, although their magnitudes are different (figure S1(*b*)). For example, some models (e.g. CARAIB, LPJ_GUESS) have larger positive trend of global GPP than the others (e.g. VEGAS), (figure S1(*b*)). In contrast to the ISIMIP2a models, MTE and MODIS estimates of global GPP show smaller long-term change over their record periods. During 1982–2010, MTE global GPP increased at a small rate of 0.08 Pg C yr^{-2}, and only Europe, Semi-arid and Arid Asia-Europe-Africa and Temperate Asia regions show a weak but significant increasing trend (figure 4). In general, the MODIS product does not show a significant trend in any region during 2000–2010, except in Tropical Asia and Tropical Africa, which have exhibit a significantly decreasing trend of −0.09 Pg C yr^{-2} and a significantly increasing trend of 0.04 Pg C yr^{-2}, respectively. In contrast, ENSEMBLE GPP during 2000–2010 showed a significant large increasing trend of 0.41 Pg C yr^{-2}, and only Temperate South America and Oceania had decreasing trends. MTE GPP during 2000–2010 generally showed similar but weaker trends as compared with ENSEMBLE GPP (figure S1(*c*)). Based on the ENSEMBLE GPP, Boreal Euro-Asia and Temperate Eastern Asia contribute most to the global GPP trend (each of them contributes about 15%), while Semi-arid and Arid Asia-Europe-Africa and Oceania contribute the least, only about 2% by each region (figure 5(*a*)).

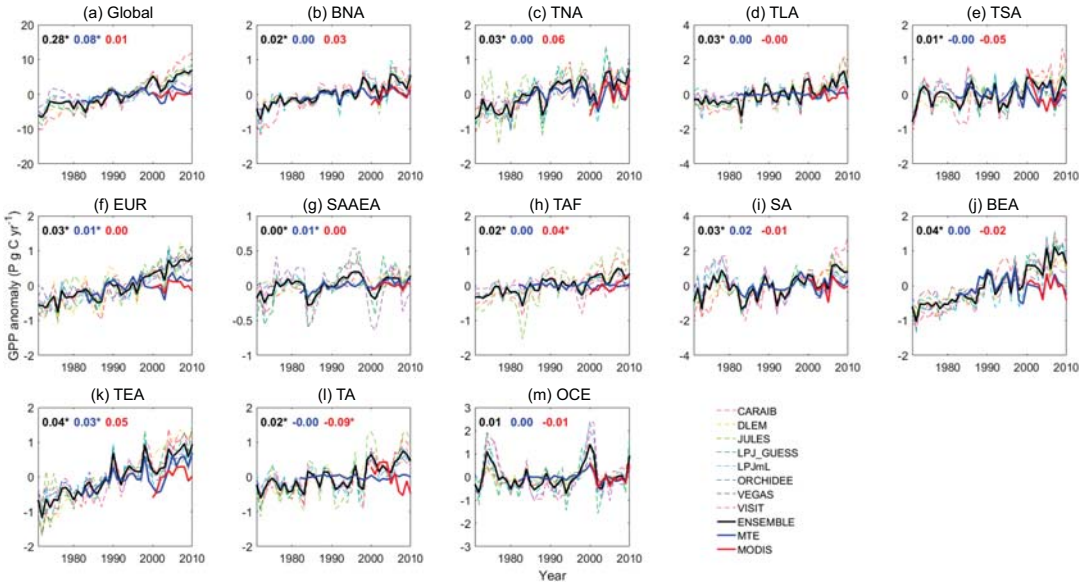

Figure 4. Inter-annual changes of global and regional GPP. The anomalies were calculated as the difference between annual GPP and the long-term mean over the period for each data source. The numbers located at the top-left corners indicate the linear trends of the ENSEMBLE (black), MTE (blue) and MODIS (red). $*$ indicate the trend is significant ($p < 0.01$).

3.3. Mean seasonality and regional contributions

Figure 6 illustrates the mean seasonal cycle of global and regional GPP. At the global scale, all datasets show similar seasonal cycles. For MODIS and ENSEMBLE, global GPP starts from as low as about 50 g C m^{-2} month^{-1} in the Northern Hemisphere (NH) winter months (i.e. December, January and February) to high values of about 100 g C m^{-2} month^{-1} in the NH summer months (i.e. June, July and August). The amplitude of MTE GPP is about 10 g C month^{-1} higher. The NH regions generally have similar seasonal patterns but higher amplitudes (as large as ~150 g C m^{-2} month^{-1}) than the global results, but the amplitudes of GPP seasonality in Semi-arid and Arid Asia-Europe-Africa are much lower than the other NH regions. There are no strong seasonal variation in tropical regions such as Tropical Latin America, Southern Africa and Tropical Asia. The Southern-Hemisphere (SH) regions of Temperate South America and Oceania show opposite patterns, which offset the higher seasonal amplitude of the NH regions resulting in the lower amplitude in seasonality of global GPP.

We found a strong correlation ($R > 0.9$) between the seasonality of ISIMIP2a models, MODIS and MTE GPP at the global scale (figures S2(*a*) and (*b*)). This varies at the regional level, however, the correlation coefficients are high in boreal and temperate regions, such as Boreal North America, Temperate North America, Temperate South America, Europe, Boreal Euro-Asia and Temperate Asia, but low in the other semi-arid, arid and tropical regions. The correlation is especially low in the Tropical Latin America, Tropical Africa and South Africa regions. In addition, the models do not agree completely on the seasonal phase of GPP in reference to MODIS and MTE products. In general, ISIMIP2a model-based seasonal phases of GPP show a positive correlation with MODIS and MTE products, but with some variations in the correlation coefficient. For example, the GPP seasonal phases estimated by JULES and CARAIB are negatively correlated with MODIS products in Tropical Latin America ($R = -0.41$ and -0.18, respectively), while the other models show positive correlations. Other examples include CARAIB and LPJ_GUESS in South Africa when compared with MODIS result in very low and negative correlations ($R = -0.14$ and -0.32, respectively), and for JULES in Tropical Latin America, LPJmL in Semi-arid and Arid Asia-Europe-Africa and South Africa, VISIT in Tropical Africa and ORCHIDEE in South Africa when compared with MTE ($R = -0.1$, -0.04, -0.03, -0.26 and -0.06, respectively).

Based on the ENSEMBLE estimates, each of the regions in the NH, including Boreal North America, Temperate North America, Europe, Boreal Euro-Asia and Temperate Asia, contributes to the global GPP seasonal variation (figure 5(*b*)) ranging from 17% to 29%. Southern Hemisphere regions (Temperate South America, South Africa and Oceania) together contribute about −14% to global GPP variability. The Semi-arid and Arid Asia-Europe-Africa and tropical regions have small contributions (−1% to 1%) to seasonal variations of global GPP. The relative regional contributions calculated from MODIS, MTE and each of the eight models support similar conclusions.

3.4. Inter-annual variability and regional contributions

During the 2000–2010 period, MODIS data suggest that the interannual variability (IAV) of global GPP was 0.8 Pg C yr^{-1}, while MTE and ENSEMBLE estimates

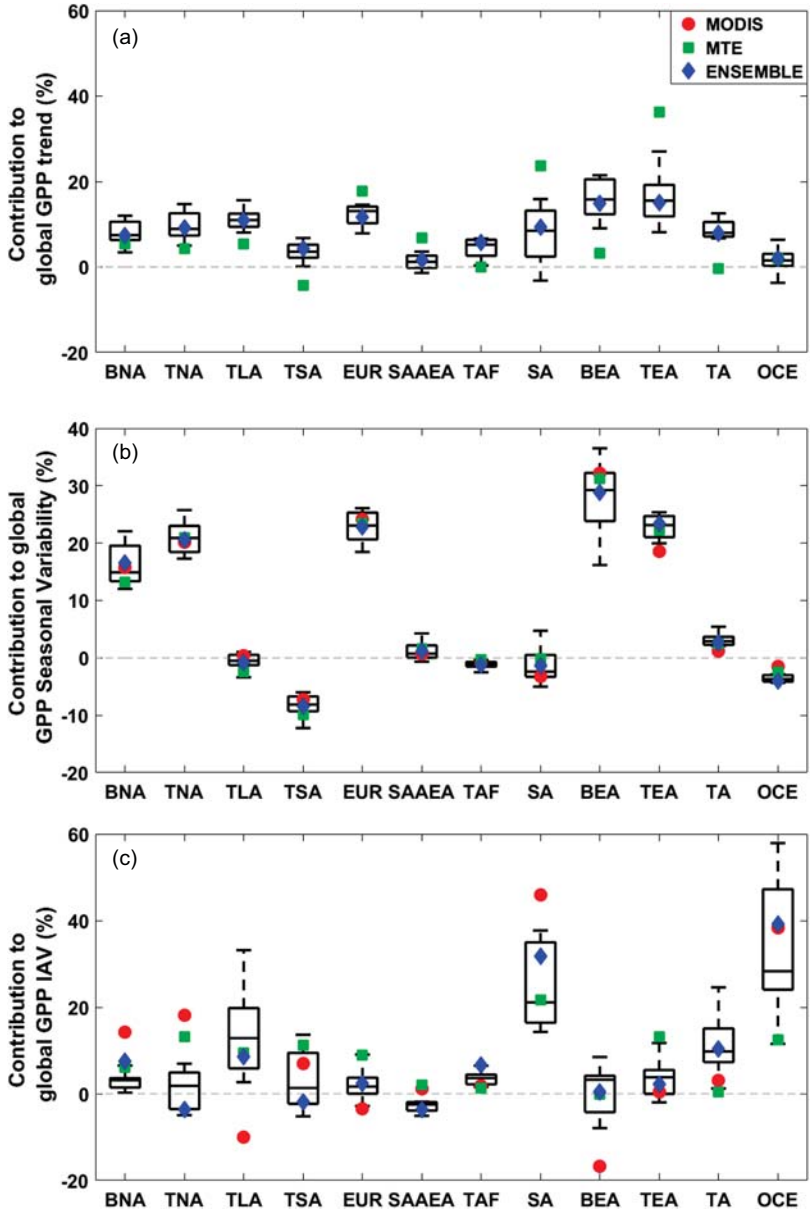

Figure 5. Regional contributions to global GPP trend, inter-annual variability (IAV), and seasonal variability. Regional contribution to global GPP trend by MODIS is not shown because MODIS GPP's global trend is too small and insignificant. Boxplots show the distributions of the eight ISIMIP models. Horizontal lines in the boxplots from top to bottom indicate the 95th, 75th, 50th, 25th, and 5th percentiles. Region abbreviations on the *x*-axes are defined in figure 1.

are nearly twice this amount (1.42 and 1.48 Pg C yr^{-1}, respectively; figure S1(*d*)). Among the regions, the ENSEMBLE generally shows the highest IAV in Boreal North America, Tropical Latin America, Semi-arid and Arid Asia-Europe-Africa, Tropical Africa, South Africa, Boreal Euro-Asia and Oceania; MODIS shows relatively higher IAV than MTE in all the regions except in Europe and Semi-arid and Arid Asia-Europe-Africa. The IAV estimates vary among ISIMIP2a models. For example, the IAV of GPP at the global scale estimated from JULES, LPJmL and VISIT are larger than 2 Pg C yr^{-1}, significantly higher than the 0.8 Pg C yr^{-1} from DLEM. At the regional scale, for example, according to LPJ_GUESS, LPJmL and VISIT the GPP in Oceania varies from 0.94 to 1.01 Pg C yr^{-1}, while it is 0.37 and 0.26 Pg C yr^{-1}, respectively, according to DLEM and JULES (figure S1(*d*)).

The correlation between the interannual variation of ISIMIP2a models, MODIS and MTE GPP at the global scale are not as good as that of the seasonality (figures S2(*c*) and (*d*)). The correlation coefficients were 0.41 and 0.57 for ENSEMBLE vs. MODIS and ENSEMBLE vs. MTE, respectively. However, the correlation coefficients are relatively high in boreal and temperate regions such as Boreal North America, Temperate North America, Semi-arid and Arid Asia-Europe-Africa, South Africa, Temperate Asia, and exceptionally high in Oceania. In contrast, the correlations are weak and even negative in some tropical regions, for example, ISIMIP2a models estimated interannual variation is

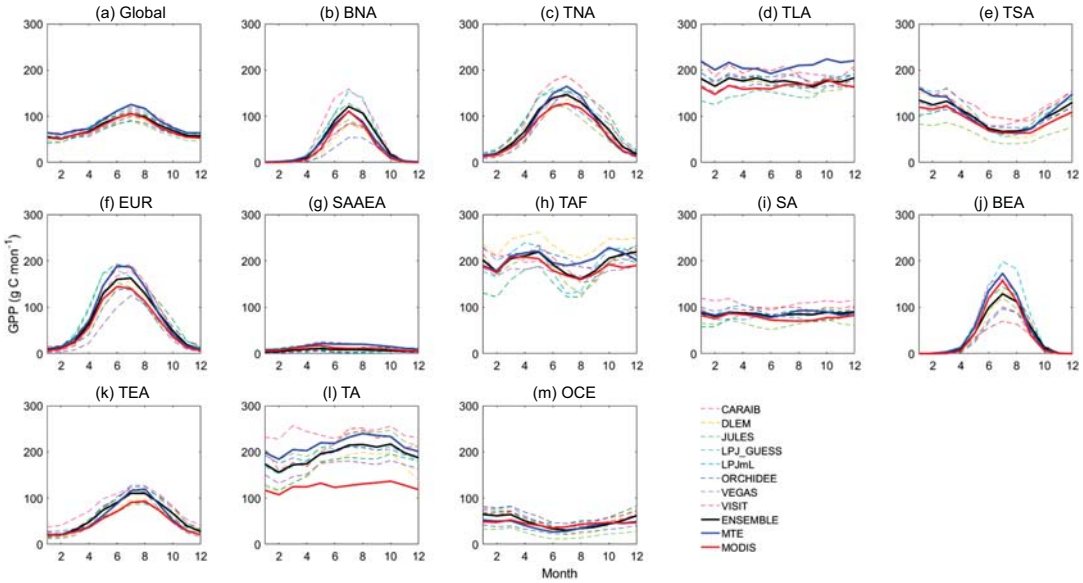

Figure 6. Mean seasonal variations in global and regional GPP for the period of each data source (MODIS: 2000–2010; MTE: 1982–2010; and ISIMIP models: 1971–2010).

negatively correlated with MODIS and MTE estimates in Tropical Africa and Tropical Africa, respectively.

Figure 5(*c*) shows the ENSEMBLE estimates of GPP for Oceania region that explains the largest fraction (39%) of IAV for global GPP, followed by South Africa (32%), Tropical Asia (10%) and Tropical Latin America (9%) regions. In contrast, the contributions of Temperate North America, Temperate South America and Semi-arid and Arid Asia-Europe-Africa regions to IAV of global GPP are negative (−2% to −4%). The remaining regions contribute relatively smaller and positive fractions to IAV of the global GPP, with Boreal Euro-Asia contributing the least (<1%). The relative regional contributions to the IAV of global GPP estimated from MODIS and MTE do not completely agree with ENSEMBLE mean values, nor with each other (figure 5(*c*)). For example, South America contributes the most to the IAV of global GPP according to MODIS and MTE data (46% and 22%, respectively); and MODIS data indicates the contributions from Tropical Latin America, Europe and Boreal Euro-Asia are negative, while all regions except Boreal Euro-Asia contribute positively based on the MTE data. There are also significant uncertainties among the estimated relative regional contributions from the eight ISIMIP2a models, especially in Tropical Latin America, South Africa and Oceania regions.

4. Discussion

In this study, we examined the spatial pattern, trends, and inter-annual and seasonal changes of global and regional GPP as simulated by the eight ISIMIP2a terrestrial biome models, and benchmarked them against observation-based MODIS and MTE GPP products. The spatial distribution and patterns of GPP based on the ISIMIP2a models ensemble mean, MODIS, and MTE all generally agree, and are consistent with other independent global GPP estimates reported in literature (Yuan *et al* 2010, Chen and Zhuang 2014, Anav *et al* 2015). The ISIMIP2a model ensemble mean is close to the mean annual GPP from MODIS and MTE, and consistent with GPP reported by Jiang and Ryu (2016) based on a mechanistic model and eddy flux data (122 ± 2.5 Pg yr^{-1} for 2001–2011). However, it is lower than the 130–169 Pg C yr^{-1} reported by the Earth system models (ESMs) simulations from the Fifth Climate Model Intercomparison Project (CMIP5) (Anav *et al* 2015); the 150–175 Pg C yr^{-1} suggested by atmospheric isotope measurements (Welp *et al* 2011); and the 146 Pg C yr^{-1} by using atmospheric CO_2 observations in a carbon cycle data assimilation system (Koffi *et al* 2012). These differences are probably due to a variety of factors such as the errors of the climate forcing in the coupled ESMs, lack of consideration of plant photorespiration in the isotope-based models, and the uncertainty of assimilation method used in the data assimilation systems (Anav *et al* 2015).

The temporal variation of global GPP based on ISIMIP2a models' estimates did not completely agree with MODIS and MTE estimates. The ISIMIP2a models show significant trends in the global and regional GPP in almost every region (except Oceania), while MODIS and MTE have few trends over their reported periods, although it is interesting to note that the MTE trend of 0.09 Pg C yr^{-2} is very close to the 1989–2008 soil respiration trend of 0.1 Pg C yr^{-2} estimated through a global synthesis (Bond-Lamberty and Thomson 2010). The overall lack of a strong GPP trend, however, is most likely due to the fact that neither MODIS nor MTE explicitly take account of CO_2

fertilization effect in their algorithms (De Kauwe *et al* 2016), despite the observed increase of atmospheric CO_2 concentration by about 1.7 ppm yr^{-1} (Conway *et al* 1994). Therefore, MODIS and MTE data do not appear to be suitable for trend analysis, as also indicated earlier by Jung *et al* (2009) and Anav *et al* (2015). In contrast, the increasing trends in model-estimated GPP appear to be consistent with other independent GPP indicators such as vegetation indices (de Jong *et al* 2012), and atmospheric carbonyl sulfide records (Campbell *et al* 2017).

Benchmarked against MODIS and MTE data, ISIMIP2a models well captured the global GPP seasonality, but they are relatively weaker in simulating the GPP seasonal cycle in the tropical regions primarily covered by tropical evergreen forests. In fact, most existing terrestrial biome models perform poorly in simulating tropical evergreen forest phenology, a key biophysical control of GPP seasonality (Kim *et al* 2012, Restrepo-Coupe *et al* 2017). Other recent studies also suggest that incorporating both the seasonal change of leaf quantity (i.e. leaf area) and quality (i.e. leaf photosynthetic capacity) can successfully explain seasonal GPP variation (Wu *et al* 2016, Wu *et al* 2017). Including this new mechanism may help the models to better simulate tropical GPP seasonality.

The IAV of GPP from MODIS, MTE and the ISIMIP2a models are generally more consistent in the temperate than in the tropical regions (figures S2(*c*) and (*d*)). One possible explanation is that IAV from MODIS and MTE in tropical regions are not as reliable as their seasonality, because some of the year-to-year change of GPP sensitivity to climate are not captured in their algorithms (Piao *et al* 2013), and the satellite-based input data are in a relatively low quality due to dense and persistent clouds in these regions (Trenberth *et al* 2001). The uncertainty of climate forcing used in ISIMIP2a models are large due to less meteorological station observations in these regions than the rest of the world, thus the models could produce inaccurate GPP estimates in these regions (Chang *et al* 2017). Another possible reason could be the poor simulation of tropical phenology in the models (Pau *et al* 2011) as indicated above. Phenology controls the length of growing season, thus being a key determinant of annual GPP (Keenan *et al* 2012, Richardson *et al* 2013, Chen *et al* 2016). Many previous studies have suggested that accurate simulation of vegetation phenology is the key to capturing IAV of the carbon cycle (Keenan *et al* 2012, Richardson *et al* 2012). We urge the modeling community to improve the phenology algorithms in their models, and to evaluate how the improved ecosystems phenology, especially in tropical regions, can help improve the IAV of regional and global GPP.

We found the regional contributions of terrestrial ecosystems to the global GPP trend, seasonality, and IAV to be generally consistent among independent methods and estimates (i.e. MODIS, MTE and ISIMIP2a models), and those reported in literature. Overall, all regions have increasing trends, and the NH regions contribute the most to the global increasing trend, mainly due to the lengthening of the growing seasons as a result of a warmer and wetter climate conditions that enhance plant growth (Piao *et al* 2007, Zhao and Running 2010). Regions in the Southern Hemisphere have smaller increasing trends, and some of the models suggest negative trend in some regions (e.g. South Africa, Oceania). This is possibly due to the increasing evaporative demand, which leads to a drying trend in these regions (Zhao and Running 2010), and reducing soil moisture (Jung *et al* 2010) and vegetation greenness (Gobron *et al* 2010). The Northern Hemisphere dominates the world's land area, and has the largest forest ecosystems, therefore, it is not surprising that it contributes the most to the seasonal variability of global GPP; and, the SH regions generally contribute negatively to it. Some tropical regions, including Tropical Latin America and Tropical Africa, cover areas that extend across the equator, therefore their net contribution are close to zero.

Our results indicate that the Oceania and South Africa regions contribute the most to the IAV of global GPP, supported by all the data sources used in this study. The dominant land cover in these regions are semi-arid savannas, grasslands and shrublands that are very sensitive to climate conditions and its variability. These findings are consistent with those previously reported by (Ahlström *et al* 2015). The IAV of GPP for these vegetation types are especially sensitive to the change of precipitation. For example, due to the periodic El Niño and La Niña events, Australia has received record high precipitation in 1975, 2000 and 2010, and experienced exceptional droughts in 1972, 1994 and 2002 (according to the data from Australian Bureau of Meteorology, www.bom.gov.au/climate/change/). The influence of these extreme events/conditions are clearly reflected in the inter-annual variation of GPP in Oceania, and our finding are consistent with previous studies (Ahlström *et al* 2015, Zhang *et al* 2016, Zscheischler *et al* 2014). In addition, the ISIMIP2a models' estimates suggest that the tropical forests in Amazonia and Southeastern Asia (regions of Tropical Latin America and Tropical Asia in this study) are the second largest contributor to the IAV of global GPP, although MODIS and MTE data do not agree with this result. There remain some debates on satellite-observed tropical forests' response to extreme climate conditions (Morton *et al* 2014, Zhou *et al* 2014, Saleska *et al* 2007, 2016), thus we cannot conclude whether the models or MTE/MODIS data are more reliable, since large-scale measurements of GPP do not exist, and terrestrial biome models show large uncertainties in these regions.

The eight ISIMIP2a model-based GPP estimates used in this study, having common climate forcing, land use and CO_2 input data were expected to provide consistent GPP estimates, especially at inter-annual and seasonal levels. However, differences relating to

the parametrization, model formulation and underlying assumptions that exist in these models appear to contribute to GPP variability, and the model ensemble approach is a good way to capture these uncertainties. It is not always clear how these assumptions propagate in the simulated parameters, especially if multiple processes are at play (Rafique *et al* 2015). Increasing complexity of models may lead to an increase in models' uncertainty associated with the introduction of new model parameters (Prentice *et al* 2015). In this study, models' simulations did not reveal a consistent set of processes behind the agreement/disagreement with MODIS and MTE GPP. Apparently, formulation of photosynthesis based on enzyme kinetics and light use efficiency (LUE) in the eight models performed equally well in simulating the inter-annual and seasonal variability of GPP. The addition of nitrogen and leaf to canopy details did not show significant influence on the GPP simulations. It is interesting that none of the models performed well in Tropical Latin America (Restrepo-Coupe *et al* 2017), suggesting that the phenological sub-models based on temperature and moisture may need further improvement. A lack of particular pattern in the models' performance does not mean that structural differences have no effect, however. For example, better parameter values of LUE and leaf to plant canopy scaling can largely improve the GPP estimates (Schaefer *et al* 2012). The number of parameters also differ widely among the eight models. Despite the differences among the eight models, the results highlight their ability to capture the importance of relative contributions of diverse ecosystems of the regions in determining the inter-annual and seasonal variability of global GPP.

5. Conclusion

The ISIMIP2a was established to foster model evaluation, and in the global biome models, how well they represent the role of terrestrial ecosystems in the carbon cycle under historical climate conditions. We used simulations from eight global terrestrial biome models participating in the ISIMIP2a to examine the spatial and temporal variability, the changes in twelve geographical regions, globally, and their contribution to the temporal variability and change in global and regional GPP. The simulated GPP from ISIMIP2a models, driven by common climate forcing, land use and CO_2 data, were 117 ± 13 Pg C yr^{-1} (model ensemble mean $\pm$ 1 standard deviation), which is in close agreement with independent global MODIS and MTE based GPP estimates. The model ensemble generally showed closer interannual variability for the higher latitudes (i.e. boreal and temperate regions) than the lower latitudes (i.e. tropical regions), while at seasonal scale, the models performed very well except in South Africa and tropical forests in Tropical Latin America and Tropical Africa regions, benchmarked against GPP estimates from MODIS and MTE. According to the model ensemble mean estimates, Tropical Latin America contributes the most to the global mean annual GPP; the regions in Asia contribute the most to the global GPP trend; the Northern Hemisphere regions dominate the global GPP seasonal variation; and Oceania is likely the largest contributor to the global GPP inter-annual variability. The results of this study provide some useful insights on the ability of the terrestrial vegetation models in capturing the spatiotemporal variability and change, and the relative contribution of twelve regions to global GPP, and its variability. These results can be used for model development/improvement, and predicting future changes in regional and global terrestrial ecosystems conditions and the models' performance as relate to the global carbon cycle, in a changing climate.

Acknowledgments

This study was funded primarily by a Laboratory Directed Research and Development project sponsored by the Pacific Northwest National Laboratory managed by Battelle Memorial Institute for the US Department of Energy. The study was also partly supported by the National Aeronautics and Space Administration Carbon Monitoring System (CMS) and ACCESS programs under projects NNH12AU35I and NNH13AW58I. The ISIMIP project is grateful for funding from the German Federal Ministry of Education and Research (BMBF, grant no. 01LS1201A1). Catherine Morfopoulos, Richard Betts and Jinfeng Chang received support from the European Commission's 7th Framework Programme (EU/FP7) under Grant Agreement 603864 (HELIX). Tian, Pan, and Yang acknowledge funding support from US National Science Foundation (1210360, 1243232), National Key Research and Development Program of China (no. 2017YFA0604700).

ORCID iDS

Ben Bond-Lamberty https://orcid.org/0000-0001-9525-4633

References

Ahlström A *et al* 2015 The dominant role of semi-arid ecosystems in the trend and variability of the land CO_2 sink *Science* **348** 895

Anav A *et al* 2015 Spatiotemporal patterns of terrestrial gross primary production: a review *Rev. Geophys.* **53** 785–818

Anav A, Friedlingstein P, Kidston M, Bopp L, Ciais P, Cox P, Jones C, Jung M, Myneni R and Zhu Z 2013 Evaluating the land and ocean components of the global carbon cycle in the CMIP5 Earth system models *J. Clim.* **26** 6801–43

Beer C *et al* 2010 Terrestrial gross carbon dioxide uptake: global distribution and covariation with climate *Science* **329** 834–8

Bond-Lamberty B and Thomson A 2010 Temperature-associated increases in the global soil respiration record *Nature* **464** 579–82

Bondeau A et al 2007 Modelling the role of agriculture for the 20th century global terrestrial carbon balance *Glob. Change Biol.* **13** 679–706

Campbell J E, Berry J A, Seibt U, Smith S J, Montzka S A, Launois T, Belviso S, Bopp L and Laine M 2017 Large historical growth in global terrestrial gross primary production *Nature* **544** 84–7

Chang J et al 2017 Benchmarking carbon fluxes of the ISIMIP2a biome models *Environ. Res. Lett.* **12** 045002

Chen M, Melaas E K, Gray J M, Friedl M A and Richardson A D 2016 A new seasonal-deciduous spring phenology submodel in the community land model 4.5: impacts on carbon and water cycling under future climate scenarios *Glob. Change Biol.* **22** 3675–88

Chen M and Zhuang Q 2014 Evaluating aerosol direct radiative effects on global terrestrial ecosystem carbon dynamics from 2003 to 2010 *Tellus B* **66** 21808

Chen M, Zhuang Q, Cook D R, Coulter R, Pekour M and Bible K 2011 Quantification of terrestrial ecosystem carbon dynamics in the conterminous United States combining a process-based biogeochemical model and MODIS and AmeriFlux data *Biogeosciences* **8** 2665–88

Ciais P et al 2013 Carbon and other biogeochemical cycles *Climate Change 2013: The Physical Science Basis. Contribution of Working Group I to the Fifth Assessment Report of the Intergovernmental Panel on Climate Change* ed T F Stocker et al (Cambridge: Cambridge University Press)

Clark D B et al 2011 The joint UK land environment simulator (JULES), model description—Part 2: carbon fluxes and vegetation dynamics *Geosci. Model Dev.* **4** 701–22

Conway T J, Tans P P, Waterman L S, Thoning K W, Kitzis D R, Masarie K A and Zhang N 1994 Evidence for interannual variability of the carbon cycle from the National Oceanic and Atmospheric Administration/Climate Monitoring and Diagnostics Laboratory Global Air Sampling Network *J. Geophys. Res. Atmos.* **99** 22831–55

Dury M, Hambuckers A, Warnant P, Henrot A, Favre E, Ouberdous M and François L 2011 Responses of European forest ecosystems to 21st century climate: assessing changes in interannual variability and fire intensity *iForest: Biogeosci. Forest.* **4** 82–99

Friedlingstein P, Cadule P, Piao S L, Ciais P and Sitch S 2010 The African contribution to the global climate-carbon cycle feedback of the 21st century *Biogeosciences* **7** 513–9

Gebremichael M and Barros A P 2006 Evaluation of MODIS gross primary productivity (GPP) in tropical monsoon regions *Remote Sens. Environ.* **100** 150–66

Gobron N, Belward A, Pinty B and Knorr W 2010 Monitoring biosphere vegetation 1998–2009 *Geophys. Res. Lett.* **37** L15402

Huntzinger D N et al 2013 The North American carbon program multi-scale synthesis and terrestrial model intercomparison project—Part 1: overview and experimental design *Geosci. Model Dev.* **6** 2121–33

Ito A and Inatomi M 2011 Water-use efficiency of the terrestrial biosphere: a model analysis focusing on interactions between the global carbon and water cycles *J. Hydrometeorol.* **13** 681–94

Jiang C and Ryu Y 2016 Multi-scale evaluation of global gross primary productivity and evapotranspiration products derived from Breathing Earth System Simulator (BESS) *Remote Sens. Environ.* **186** 528–47

de Jong R, Verbesselt J, Schaepman M E and de Bruin S 2012 Trend changes in global greening and browning: contribution of short-term trends to longer-term change *Glob. Change Biol.* **18** 642–55

Jung M, Reichstein M and Bondeau A 2009 Towards global empirical upscaling of FLUXNET eddy covariance observations: validation of a model tree ensemble approach using a biosphere model *Biogeosciences* **6** 2001–13

Jung M et al 2010 Recent decline in the global land evapotranspiration trend due to limited moisture supply *Nature* **467** 951–4

Jung M et al 2011 Global patterns of land-atmosphere fluxes of carbon dioxide, latent heat, and sensible heat derived from eddy covariance, satellite, and meteorological observations *J. Geophys. Res. Biogeosci.* **116** G00J07

Jung M, Verstraete M, Gobron N, Reichstein M, Papale D, Bondeau A, Robustelli M and Pinty B 2008 Diagnostic assessment of European gross primary production *Glob. Change Biol.* **14** 2349–64

De Kauwe M G, Keenan T F, Medlyn B E, Prentice I C and Terrer C 2016 Satellite based estimates underestimate the effect of CO_2 fertilization on net primary productivity *Nat. Clim. Change* **6** 892–3

Keenan T F, Davidson E, Moffat A M, Munger W and Richardson A D 2012 Using model-data fusion to interpret past trends, and quantify uncertainties in future projections, of terrestrial ecosystem carbon cycling *Glob. Change Biol.* **18** 2555–69

Kim Y, Knox R G, Longo M, Medvigy D, Hutyra L R, Pyle E H, Wofsy S C, Bras R L and Moorcroft P R 2012 Seasonal carbon dynamics and water fluxes in an Amazon rainforest *Glob. Change Biol.* **18** 1322–34

Koffi E N, Rayner P J, Scholze M and Beer C 2012 Atmospheric constraints on gross primary productivity and net ecosystem productivity: Results from a carbon-cycle data assimilation system *Glob. Biogeochem. Cycles* **26** GB1024

Krinner G, Viovy N, de Noblet-Ducoudré N, Ogée J, Polcher J, Friedlingstein P, Ciais P, Sitch S and Prentice I C 2005 A dynamic global vegetation model for studies of the coupled atmosphere-biosphere system *Glob. Biogeochem. Cycles* **19** GB1015

Lee J-E et al 2013 Forest productivity and water stress in Amazonia: observations from GOSAT chlorophyll fluorescence *Proc. R. Soc.* B **280** 20130171

Liu D, Cai W, Xia J, Dong W, Zhou G, Chen Y, Zhang H and Yuan W 2014 Global validation of a process-based model on vegetation gross primary production using eddy covariance observations *PLoS One* **9** e110407

Ma J, Yan X, Dong W and Chou J 2015 Gross primary production of global forest ecosystems has been overestimated *Sci. Rep.* **5** 10820

Morton D C, Nagol J, Carabajal C C, Rosette J, Palace M, Cook B D, Vermote E F, Harding D J and North P R J 2014 Amazon forests maintain consistent canopy structure and greenness during the dry season *Nature* **506** 221–4

Nightingale J M, Fan W, Coops N C and Waring R H 2008 Predicting tree diversity across the United States as a function of modeled gross primary production *Ecol. Appl.* **18** 93–103

Pan S et al 2014 Complex spatiotemporal responses of global terrestrial primary production to climate change and increasing atmospheric CO_2 in the 21st century *PLOS ONE* **9** e112810

Pau S, Wolkovich E M, Cook B I, Davies T J, Kraft N J B, Bolmgren K, Betancourt J L and Cleland E E 2011 Predicting phenology by integrating ecology, evolution and climate science *Glob. Change Biol.* **17** 3633–43

Piao S, Friedlingstein P, Ciais P, Viovy N and Demarty J 2007 Growing season extension and its impact on terrestrial carbon cycle in the Northern Hemisphere over the past 2 decades *Glob. Biogeochem. Cycles* **21** GB3018

Piao S et al 2013 Evaluation of terrestrial carbon cycle models for their response to climate variability and to CO_2 trends *Glob. Change Biol.* **19** 2117–32

Prentice I C, Liang X, Medlyn B E and Wang Y-P 2015 Reliable, robust and realistic: the three R's of next-generation land-surface modelling *Atmos. Chem. Phys.* **15** 5987–6005

Le Quéré C et al 2016 Global carbon budget 2016 *Earth Syst. Sci. Data* **8** 605–49

Rafique R, Kumar S, Luo Y, Kiely G and Asrar G 2015 An algorithmic calibration approach to identify globally optimal parameters for constraining the DayCent model *Ecol. Modell.* **297** 196–200

Restrepo-Coupe N et al 2017 Do dynamic global vegetation models capture the seasonality of carbon fluxes in the Amazon basin? A data-model intercomparison *Glob. Change Biol.* **23** 191–208

Richardson A D *et al* 2012 Terrestrial biosphere models need better representation of vegetation phenology: results from the North American carbon program site synthesis *Glob. Change Biol.* **18** 566–84

Richardson A D, Keenan T F, Migliavacca M, Ryu Y, Sonnentag O and Toomey M 2013 Climate change, phenology, and phenological control of vegetation feedbacks to the climate system *Agric. Forest Meteorol.* **169** 156–73

Running S W, Nemani R R, Heinsch F A, Zhao M, Reeves M and Hashimoto H 2004 A continuous satellite-derived measure of global terrestrial primary production *Bioscience* **54** 547–60

Saleska S R, Didan K, Huete A R and da Rocha H R 2007 Amazon forests green-up during 2005 drought *Science* **318** 612

Saleska S R, Wu J, Guan K, Araujo A C, Huete A, Nobre A D and Restrepo-Coupe N 2016 Dry-season greening of Amazon forests *Nature* **531** E4–5

Schaefer K *et al* 2012 A model-data comparison of gross primary productivity: results from the North American carbon program site synthesis *J. Geophys. Res. Biogeosci.* **117** G03010

Sitch S *et al* 2008 Evaluation of the terrestrial carbon cycle, future plant geography and climate-carbon cycle feedbacks using five dynamic global vegetation models (DGVMs) *Glob. Change Biol.* **14** 2015–39

Sjöström M *et al* 2013 Evaluation of MODIS gross primary productivity for Africa using eddy covariance data *Remote Sens. Environ.* **131** 275–86

Smith B, Prentice I C and Sykes M T 2001 Representation of vegetation dynamics in the modelling of terrestrial ecosystems: comparing two contrasting approaches within European climate space *Glob. Ecol. Biogeogr.* **10** 621–37

Tian H *et al* 2015 North American terrestrial CO_2 uptake largely offset by CH_4 and N_2O emissions: toward a full accounting of the greenhouse gas budget *Clim. Change* **129** 413–26

Tian H, Xu X, Liu M, Ren W and Zhang C 2010 Spatial and temporal patterns of CH_4 and N_2O fluxes in terrestrial ecosystems of North America during 1979–2008: application of a global biogeochemistry model *Biogeosciences* **7** 2673–94

Trenberth K E, Stepaniak D P, Hurrell J W and Fiorino M 2001 Quality of reanalyses in the tropics *J. Clim.* **14** 1499–510

Turner D P *et al* 2006 Evaluation of MODIS NPP and GPP products across multiple biomes *Remote Sens. Environ.* **102** 282–92

Warszawski L, Frieler K, Huber V, Piontek F, Serdeczny O and Schewe J 2014 The Inter-Sectoral Impact Model Intercomparison Project (ISI–MIP): project framework *Proc. Natl Acad. Sci.* **111** 3228–32

Welp L R, Keeling R F, Meijer H A J, Bollenbacher A F, Piper S C, Yoshimura K, Francey R J, Allison C E and Wahlen M 2011 Interannual variability in the oxygen isotopes of atmospheric CO_2 driven by El Nino *Nature* **477** 579–82

Wu J *et al* 2016 Leaf development and demography explain photosynthetic seasonality in Amazon evergreen forests *Science* **351** LP-972–76

Wu J, Serbin S P, Xu X, Albert L P, Chen M, Meng R, Saleska S R and Rogers A 2017 The phenology of leaf quality and its within-canopy variation is essential for accurate modeling of photosynthesis in tropical evergreen forests *Glob. Change Biol.* (https://doi.org/10.1111/gcb.13725)

Xia J *et al* 2015 Joint control of terrestrial gross primary productivity by plant phenology and physiology *Proc. Natl Acad. Sci.* **112** 2788–93

Yuan W *et al* 2010 Global estimates of evapotranspiration and gross primary production based on MODIS and global meteorology data *Remote Sens. Environ.* **114** 1416–31

Zeng N, Qian H, Roedenbeck C and Heimann M 2005 Impact of 1998–2002 midlatitude drought and warming on terrestrial ecosystem and the global carbon cycle *Geophys. Res. Lett.* **32** L22709

Zhang Y *et al* 2016 Precipitation and carbon-water coupling jointly control the interannual variability of global land gross primary production **6** 39748

Zhao M and Running S W 2010 Drought-induced reduction in global terrestrial net primary production from 2000 through 2009 *Science* **329** 940–3

Zhou L, Tian Y, Myneni R B, Ciais P, Saatchi S, Liu Y Y, Piao S, Chen H and Hwang T 2014 Widespread decline of Congo rainforest greenness in the past decade *Nature* **509** 86–90

Zhu H, Lin A, Wang L, Xia Y and Zou L 2016 Evaluation of MODIS gross primary production across multiple biomes in China using eddy covariance flux data *Remote Sens.* **8** 395

Zscheischler J *et al* 2014 A few extreme events dominate global interannual variability in gross primary production *Environ. Res. Lett.* **9** 35001